III INTERNATIONAL CONGRESS

ALICANTE · 2026



THE BRAIN AND THE CHIP

IMPLANTABLE BRAIN–COMPUTER INTERFACES

Poster abstract programme

- **A** Visual processing and neural coding
- **B** Neural mechanisms of artificial vision
- **C** Prosthetic vision perception and rehabilitation
- **D** Neural interfaces stimulation technology and biocompatibility
- **E** Neural decoding brain machine interfaces and research tools
- **F** Neuroethics neurorights and legal responsibility

26–28 OCT 2026

Alicante, Spain

26–28 October 2026

Poster Index

SECTION A Visual processing and neural coding

P01 Matthias Baumann Figuring Out More About Figure-Ground Segregation: the Contribution of the Superior Colliculus

P02 Aleksejs Timčenko Low-Dimensional Population Codes for Natural Videos In Mouse Superior Colliculus

P03 Yong Sook Goo Enhanced Correlated RGC Firing and Abnormal Rhythm in Retinal Detachment

P04 Radovan Vodila A Third Dimension of the V1 Orientation Manifold Makes Cardinality Explicit

P05 Rubén Pérez-Elvira Toward a Common Cortical Grammar: Stimulus-Dependent Geometry Across Visual Areas

SECTION B Neural mechanisms of artificial vision

P06 Matthieu Provansal Two-Photon Imaging of Electrical Microstimulation-Induced Neuronal Activity Patterns in Mouse V1.

P07 Corinne Orlemann Neural Activation Patterns of SST, PV, and VIP Interneurons to Microstimulation Parameters in the Mouse Primary Visual Cortex

P08 Adrián Villamarín-Ortiz Network State Predicts Bidirectional Reconfiguration Across Intracortical Stimulation Sessions in Human Visual Cortex

P09 Odelaisys Hernández-Echevarría Multimodal Responses Recorded with a Utah Array in the Visual Cortex of an Early-Blind Participant

P10 María Ángeles Martínez-Gilabert High-Density EEG Characterization of the Somatosensory N20 and Resting-State Alpha Activity in Participants with Visual Impairment: Preliminary Findings

P11 Feng Wang High-Density Recording and Microstimulation of the Macaque Lateral Geniculate Nucleus

P12 Puk Lavreeke Nuijten From Thalamic Stimulation to Perception: Cortical and Perceptual Detection Responses to Electrical Activation of the LGN

P13 Rim Sadry Visual Coding and Artificial Activation in the LGN–V1 Pathway

P14 Prithu Purkait Optogenetic Stimulation in the Macaque Lateral Geniculate Nucleus: Acute Electrophysiological Validation

SECTION C Prosthetic vision perception and rehabilitation

P15 Lillian Isabel Ocampo Fernández PhosLab: A Computational Platform for Phosphene Mapping in Cortical Visual Implants Using Anatomical Models and AI

P16 Estela Díaz-López Security-Aware Scenario-Based Operational Vocabulary

P17 Maureen van der Grinten An Augmented Reality Platform for Comparing Simulated and Actual Prosthetic Vision

P18 María del Mar Ayuso Arroyave Neurovision: A wireless Virtual Reality Platform for Mobility-Oriented Prosthetic Vision Simulation

P19 Ashkan Rahmani Nejad Point-SPV: end-to-end Enhancement of Object Recognition in Simulated Prosthetic Vision Using Synthetic Viewing Points

P20 Eleftherios Papadopoulos The Impact of a Linear Ground Texture on Distance Estimation in Simulated Phosphene Vision

P21 Félix de la Paz López Blind People Guidance Using Area Center Algorithm

P22 María del Mar Ayuso Arroyave Oculomotor Stability Predicts Phosphene Perception in a Blind Participant with Cortical Visual Neuroprosthesis

P23 Elena von Perponcher Crowding at an Eccentric Locus: Location-Specific Perceptual Learning And Its Implications for Visual Rehabilitation After Implantation

Poster index continued

SECTION D Neural interfaces stimulation technology and biocompatibility

P24 Emilie Revol Towards a Flexible, Deep, High-Channel-Count Electrode Array for Cortical Visual Prosthetics

P25 Lucía Navarro-González Inter-Shank Spacing as a Key Factor in the Spatial Organization of Cortical Tissue Responses to Flexible Intracortical Electrodes

P26 Gloria Ruiz-Boix Changes in Myelin Morphology Following Penetrating Electrode Array Implantation in Peripheral Nerves.

P27 Peimin Yuan Hybrid Electrical and Optical Visual Cortical Prosthesis

P28 Xiyuan He Closed-Loop Neural Stimulation for Visual Prosthetics

P29 Marta Gea Ponce A Hardware-Enforced Safety Envelope for Ml-Driven Intracortical Stimulation

P30 Julia Paredes de Isla HEMI-FLASH-RED: a Red-LED Flash VEP Stimulator With Hemifield Stimulation and EEG Synchronisation

SECTION E Neural decoding brain machine interfaces and research tools

P31 Alessia Sepe Beyond Simple Movements: Premotor Cortex Enables Adaptive BMI Control

P32 Lorenzo Russo ImaDec: Visual Imagery Decoding from V1 of a Blind Participant

P33 Diogo Berger Monteiro Learning Continuous Representation from Raw Intracortical Recordings

P34 Ryan Greer Embedded Deep Learning Models Towards Low-Power Neural Interfaces

P35 Paolo Papale BigParma: An Open-Source Package for Fast and Automated Probe Planning and Implant Modeling.

P36 Kristian Gjorgjieski Generalizable Deep Learning Models for Predicting Auditory Neural Responses

P37 David Beinhauer Can Shared Neural Responses Be Found Without Knowing Where to Look?

P38 Sofía Cabrera ENGRAM: a Synchronised Platform For Neural And Media Data Visualisation

P39 Geraldin Sthefany Saavedra Tafur Multimodal Platform for MRI-Guided TMS Data Integration and 3D Visualization in Phosphene Research.

SECTION F Neuroethics neurorights and legal responsibility

P40 Marcin Furtak The Problem of Responsibility Gap in AI-Based Assistive Technology

P41 María Remedios Guilabert Vidal PROTECTING NEURODATA: Neurorights Liability Under Article 82 of the GDPR and Other Instruments

P42 María Concepción Rayón Ballesteros De las Señales Neuronales a la Prueba Jurídica: Neuroderechos y Garantías Procesales ante las Interfaces Cerebro-Computador Intracorticales

SECTION A / Visual processing and neural coding

P01

Figuring Out More About Figure-Ground Segregation: the Contribution of the Superior Colliculus

Presenter Matthias Baumann

One of the most important tasks of the visual system is to segregate objects from their backgrounds to guide behavior, a process called figure-ground segregation (FGS). FGS is thought to require both early local mechanisms, like edge detection, and later global mechanisms for grouping features that belong to the same object. Neural correlates of FGS have been found in cortical visual areas as early as the primary visual cortex (V1). Neurons of macaque monkeys showed enhanced responses to figures compared to backgrounds, an effect known as figure-background modulation (FBM). This has been taken as evidence that feedback from higher visual areas influences activity in early visual areas, in which neurons have small receptive fields (RFs). What is yet unknown is how the FBM signal in visual areas is transformed into a motor response in lower areas in order to make eye movements towards these segregated objects. In this study, we investigated the role of the subcortical superior colliculus (SC) in this sensory-motor transformation during FGS. Using single electrodes, we measured activity in SC in response to various figure-ground stimuli. We found that SC showed figure-background modulation, already on a single-cell level. Interestingly, FBM was faster and occurred on a larger spatial scale than FBM that has been previously found in V1. Furthermore, we found that within SC itself, across the different SC layers, a transformation from a visual object representation into a motor response occurred. The superficial layers showed a detailed representation of the entire figure, including the boundaries, which over time was transformed into a more global center response in deep layers, to guide eye movements towards the figure center. This suggests that SC is part of an evolutionarily preserved system that can quickly detect salient stimuli, that might be able to bypass the cortex and enable fast eye movements towards these stimuli. Later in time, SC probably interacts with the visual and frontal cortex to accomplish a more detailed view of the stimulus and guide more cognitive behavior accordingly.

SECTION A / Visual processing and neural coding

P02

Low-Dimensional Population Codes for Natural Videos In Mouse Superior Colliculus

Presenter Aleksejs Timčenko

Visual system represents and compresses high-dimensional inputs from natural environments. Despite their complexity, natural stimuli have strong statistical structure including pixel inten-sity correlations. At the same time, neural activity is organized at the population level through shared stimulus drive and correlated variability, limiting how far single-neuron receptive-field descriptions can take us. Here we ask how natural video streams are encoded by retinal inputs to mouse superior colliculus (SC), and whether stimulus and response structure can be used to uncover a robust low-dimensional population code. We analyze functional calcium imaging (GCaMP8) of retinal axons in SC during presentation of 10 second natural video clips. We first characterize low-dimensional structure in population responses using principal component analysis (PCA), and then link stimulus features to response latents using low-rank stimulus-response models (CCA/RRR), interpreting the resulting weights and loadings as population-level basis functions. Population responses to natural videos concentrate in a compact and interpretable latent space, which explains a significant fraction of stimulus-driven variance. The recovered basis patterns are highly structured, resembling Fourier-like spatial features rather than collec-tions of independent center-surround receptive fields, suggesting a genuinely population-level representation. Thus, encoding models with a low-dimensional bottleneck show promise in characterizing processing of dynamic natural world in the early visual system.

SECTION A / Visual processing and neural coding

P03

Enhanced Correlated RGC Firing and Abnormal Rhythm in Retinal Detachment

Presenter Yong Sook Goo

Yong Sook Goo[1], Dae Jin Park[1]
[1]Chungbuk National University College of Medicine, Physiology, Cheongju, Republic of Korea

Purpose: Metamorphopsia and blurred vision often persist despite anatomically successful retinal detachment (RD) repair. We investigated time-dependent structural and functional alterations in retinal network activity following RD.

Methods: RD was induced in adult C57BL/6J mice by trans-scleral subretinal sodium hyaluronate injection. Eyes were collected on post-RD days 1, 3, 7, and 14. Optical coherence tomography and hematoxylin–eosin staining were used to verify structural changes. Retinal ganglion cell (RGC) activity was recorded using an 8 × 8 multielectrode array.

Network alterations were assessed using the cross-correlation index (CCI) of RGC spike pairs, power spectral density (PSD), and continuous wavelet transform analyses. CCIs were decomposed into narrow (<10 ms), medium (10–50 ms), and broad (>100 ms) correlations to infer the underlying sources of correlated RGC activity and assess their changes following RD. The gap-junction blocker meclofenamic acid (MFA) was applied to evaluate the contribution of electrical coupling.

Results: RD produced early outer-retinal edema followed by progressive retinal atrophy. Spontaneous RGC activity exhibited enhanced medium-range correlations at post-RD days 7 and 14, with the strongest increase observed at day 14, whereas narrow-timescale spike synchrony was not significantly altered.

Log-scale PSD analysis demonstrated increased 5–10 Hz oscillatory power at later RD stages. MFA reduced both oscillatory power and medium-range correlation.

Conclusions: RD is associated with progressive structural changes and altered retinal network activity characterized by enhanced medium-range correlation and low-frequency oscillatory rhythms, consistent with involvement of gap-junction–dependent inner retinal circuitry. These findings support the possibility that functional retinal remodeling contributes to persistent visual dysfunction after RD.

SECTION A / Visual processing and neural coding

P04

A Third Dimension of the V1 Orientation Manifold Makes Cardinality Explicit

Presenter Radovan Vodila

Radovan Vodila[1] , Antonio Lozano[2] , Katja Seeliger[3] , Eduardo Fernández[2] , Richard van Wezel[1]
[1]Donders Institute for Brain, Cognition and Behaviour, Radboud University, Nijmegen, The Netherlands
[2]Bioengineering Institute and Cátedra Bidons Egara, University Miguel Hernández, Elche, Spain
[3]Max Planck Institute for Human Cognitive and Brain Sciences, Leipzig, Germany

Orientation is encoded as a circular variable in primary visual cortex (V1), but the geometry of its population representation remains incompletely understood. Behavioural and neuroimag- ing studies report differences between horizontal and vertical (cardinal) orientations, and obliques. Existing accounts relate these anisotropies to neuronal tuning, originating from en- vironmental statistics, and perceptual priors. Accounts anchored at the level of local precision, however, do not uniquely determine the representational geometry of population responses. Representational format constrains the computations through which downstream circuits can extract encoded information. Following the principle of representational untangling, we asked whether the macaque V1 population code makes cardinality linearly explicit: accessible to a common linear readout across category-preserving changes in orientation. Using demixed principal component analysis of macaque V1 multi-unit responses to natural images, we identified an additional cardinal-phase coordinate accompanying the orientation ring manifold. In responses to held-out images, the ring coordinates supported readout of orientation identity, whereas the cardinal coordinate supported a linear readout of cardinality across orthogonal orientation pairs. Cardinality was also recoverable through a nonlinear transformation of the ring coordinates, showing that the additional coordinate made existing category information accessible to a linear readout. We then used encoding-model inversion to replicate the findings and test whether the identified coordinates could guide targeted stimulus design. Synthesized images shifted predicted cardinal scores relative to matched controls while approximately preserving represented orientation. This provides concrete predictions for manipulating these population coordinates through visual input. In sum, these findings support cardinality as an explicit, linearly accessible feature of V1 population activity.

SECTION A / Visual processing and neural coding

P05

Toward a Common Cortical Grammar: Stimulus-Dependent Geometry Across Visual Areas

Presenter Rubén Pérez-Elvira

Rubén Pérez-Elvira, Carlos Aznárez, Álvaro García-Lajara, Daniel Cordeiro, María Agudo Juan, David Wöbbeking

Some theories have proposed that the neocortex contains repeated local circuit motifs (Mountcastle, 1997), yet demonstrating a shared computational principle requires moving from anatomy to an observable population-level measure. We adopted a geometric approach: if several areas share an organizational principle, they need not produce identical neural responses, but could preserve similar structural relationships across stimulus conditions. We hypothesized that visual areas apply area-specific transformations to sensory input while still retaining a partially shared latent geometry. Using two-photon calcium imaging from the Allen Brain Observatory Visual Coding dataset (mouse), we analyzed five visual areas (VISp, VISl, VISal, VISpm, VISam) across four stimulus families (natural movies, natural scenes, drifting gratings). We combined representational similarity analysis (RDMs via correlation distance), within-area decoding (SVM, logistic regression, random forest; trial caps of 40/80/120), cross-area transfer after PCA + Procrustes alignment, and principal-angle comparison of latent subspaces, integrated into a shared-geometry index (SGI). Inter-area RDM correlation was stimulus-dependent: natural movies showed more consistent cross-area geometry than static scenes (10/10 vs. 1/10 significant pairs), and the movie-vs-scene decoding gap widened with more trials (0.18→0.28). Geometry induced by natural movies transferred across areas after latent alignment (balanced accuracy 0.34 vs.~0.01 for scenes). A shared-latent-geometry model ($X_i \approx Z \cdot W_i + \varepsilon_i$) fit best for drifting gratings and natural movies (SGI 0.81 and 0.58; mean R^2 0.48 and 0.32) and worst for static scenes (SGI 0.12). These findings support neither a strictly universal cortical code nor a purely localist view, but an intermediate position: visual areas are functionally specialized yet can share geometric regularities that emerge in a stimulus-dependent manner, providing an empirical, measurable operationalization of Mountcastle's columnar-motif intuition.

SECTION B / Neural mechanisms of artificial vision

P06

Two-Photon Imaging of Electrical Microstimulation-Induced Neuronal Activity Patterns in Mouse V1.

Presenter Matthieu Provansal

Matthieu Provansal, Corinne Orlemann, Paul Neering, Claudio Ray, Patrick Ruther, Maria Asplund, Pieter Roelfsema

Brain machine interfaces represent a promising technology to restore sight in blind individuals. These devices rely on intracortical electrodes which activate the surrounding neurons, leading to the perception of artificial dots of light. Many parameters can shape the electrical stimulation and therefore impact the neuronal activation spread and corresponding visual percept. We therefore need to understand how these parameters control the activated neuronal population.

To this end, we have developed a pipeline combining electrical microstimulation and 2-photon imaging in mice to compare the excitatory neurons activation patterns elicited by different stimulation parameters.

Among those parameters, double electrode bipolar stimulation steers the current between electrodes compared to double electrode monopolar stimulation. Our results show this current steering does not segregate the activity between the electrodes. Instead, the main changes triggered by bipolar stimulation resides in the decrease of neuronal activation associated with the switch of one cathode-leading electrode to an anode-leading electrode.

This work has important implications for the development of next-generation visual prosthetics.

SECTION B / Neural mechanisms of artificial vision

P07

Neural Activation Patterns of SST, PV, and VIP Interneurons to Microstimulation Parameters in the Mouse Primary Visual Cortex

Presenter Corinne Orlemann

Intracortical microstimulation of sensory brain areas is a promising approach for brain-computer interfaces. In the visual cortex, microstimulation evokes phosphenes (i.e., small dots of light), which can serve as a basis of artifical vision. However, unlike optogenetic stimulation, microstimulation is not cell type-specific and activates entire neural circuits, including both excitatory and inhibitory neurons that shape sensory perception. Previous studies have also reported adaptation effects that reduce stimulation efficacy over time, likely due to the accumulation of inhibitory activity. Despite this, there remains limited knowledge on how specific interneuron subtypes respond to different stimulation parameters. Here, we investigated the effects of microstimulation on PV, SST, and VIP interneurons by combining electrical microstimulation with two-photon imaging in mice. We examined the effects of phase polarity, pulse frequency, and stimulation amplitude during single-electrode stimulation, as well as monopolar and bipolar configurations in multi-electrode paradigms. To investigate the role of interneurons in adaptation, we also analyzed neural responses across repetitive stimulation trials. Preliminary results show that all interneuron subtypes respond more strongly to cathode-leading than anode-leading stimulation, consistent with previous findings in excitatory neurons. SST neurons exhibited lower activation thresholds than PV and VIP neurons and preferentially responded to higher stimulation frequencies, whereas responses at 50 Hz were reduced. In addition, SST neurons showed broader spatial activation, while PV neuron responses were concentrated around the stimulation electrode. VIP neurons displayed the lowest response rates to microstimulation.

SECTION B / Neural mechanisms of artificial vision

P08

Network State Predicts Bidirectional Reconfiguration Across Intracortical Stimulation Sessions in Human Visual Cortex

Presenter Adrián Villamarín-Ortiz

Adrián Villamarin-Ortiz[1], Fabrizio Grani[2], L. Soo[1], Rocio Lopez Peco[2], A. Kovalev[1], L. Navarro-González[1], G. Ruiz-Boix[1], O. Hernández-Echevarria[1], M. M. Ayuso Arroyave[1], A. Bernabeu[1], A. Lozano[3], C. Soto-Sanchez[1], E. Fernández Jover[1]

The effects of intracortical stimulation depend not only on how stimulation is delivered, but also on the ongoing state of the cortical network. Whether this state dependence shapes network-level responses to repeated stimulation in humans remains unclear. Here, we examined how resting-state population activity in human V1 changes following intracortical microstimulation, using 216 recording sessions from five blind participants with chronically implanted microelectrode arrays. Across sessions, cortical coupling changed bidirectionally following stimulation, reflecting structured reconfiguration of network interactions rather than uniform shifts or ordinary within-recording variability. The prestimulation network state predicted whether coupling subsequently increased or decreased, and this relationship generalized across participants in leave-one-participant-out prediction. Reorganization also showed spatial and longitudinal organization: changes in network hubs recurred within reproducible cortical territories, showed spatial relationships with stimulated electrodes, and overlapped descriptively with percept-relevant sites. Over longer timescales, cumulative stimulation history was associated with the prestimulation network state, consistent with a carryover of prior stimulation into subsequent sessions. By contrast, the amount of stimulation delivered within a given session provided little additional information about the acute network response once the prestimulation state was taken into account. Together, these findings support a state-dependent view of chronic intracortical stimulation in which prior stimulation can shape the network state carried into a session, and that state in turn influences how the cortex responds to new stimulation. Accounting for this evolving network state may therefore improve the interpretation and design of chronic intracortical stimulation protocols. More broadly, these results suggest that state-aware stimulation strategies could help make cortical neuroprosthetic interventions more consistent and predictable over time.

SECTION B / Neural mechanisms of artificial vision

P09

Multimodal Responses Recorded with a Utah Array in the Visual Cortex of an Early-Blind Participant

Presenter Odelaisys Hernández-Echevarría

Odelaisys Hernández-Echevarría[1]*, Gloria Ruiz-Boix[1]*, Antonio Lozano[1], Lucía Navarro-González[1], Aleksandr Kovalev[1], María Ángeles Martínez-Gilabert, María del Mar Ayuso Arroyave[1], Adrián Villamarin-Ortiz[1], Ángela Bernabeu-Sanz[1], Leili Soo[1], Cristina Soto-Sánchez[1] and Eduardo Fernández[1,2]

[1]Biomedical Neuroengineering Group (nBio), Instituto de Bioingeniería (IB), Universidad Miguel Hernández (UMH), 03202, Elche, Spain

[2] Research Networking Center in Bioengineering, Biomaterials and Nanomedicine (CIBER-BBN), 28029, Madrid, Spain

* These authors contributed equally (gloria.ruiz@goumh.umh.es and o.hernandez@umh.es)

Introduction: Long-term visual deprivation may alter how visual cortex responds to sensory inputs. We examined local field potentials (LFPs) and spiking responses to visual, auditory and somatosensory stimulation in a participant with early-onset blindness.

Methods: This exploratory single-case study involved a woman with early-onset blindness of 60 years duration. She retains light perception in the left eye but none in the right. A 96-electrode Utah array was implanted in the right primary visual cortex (V1). Ganzfeld flashes were presented to the left eye at 1.5, 3, 10 and 30 cd/m² and to the right eye at 3, 10, 30 and 60 cd/m² during passive viewing and detection tasks. Each ear received auditory stimulation using two oddball paradigms: a passive mismatch negativity (MMN) and an active P300 in which rare tones were counted. Each median nerve was stimulated at the minimum intensity producing thumb movement. We analyzed stimulus-locked LFPs, multi-unit activity (MUA; 500–1500 Hz) and spikes from sorted units.

Results: Flash detection increased with luminance for the left eye and remained low for the right. Visual LFPs did not show a clear canonical evoked waveform. Left-eye stimulation was associated with late activity (200–1500 ms), with higher MUA during detection than during passive viewing (+1.3 percentage points across recordings; $p < 0.001$). Auditory deviant tones produced LFP differences and increases in late MUA and summed firing activity; significant firing contrasts in that session were approximately 10–13% ($p \leq 0.013$). In the pooled analysis across six recording time points, active oddball stimulation showed positive deviant–standard effects in MUA and firing activity, whereas passive oddball effects were not significant. Median nerve stimulation produced an early LFP deflection, without consistent population MUA or short-latency single-unit responses.

Conclusions: Late visual activity was associated with the light-perceiving eye and the detection task, potentially reflecting task-related processing of residual visual perception. Responses to auditory deviant tones, particularly during active counting, support possible nonvisual modulation of activity recorded in V1. Somatosensory stimulation elicited LFP deflections without consistent modulation of spiking activity, leaving their local neuronal origin unresolved. These preliminary findings provide the basis for further investigation of sensory modulation in visual cortex after prolonged blindness.

SECTION B / Neural mechanisms of artificial vision

P10

High-Density EEG Characterization of the Somatosensory N20 and Resting-State Alpha Activity in Participants with Visual Impairment: Preliminary Findings

Presenter María Ángeles Martínez-Gilabert

María Ángeles Martínez-Gilabert[1]*, Odelaisys Hernández-Echevarría[1]*, Gloria Ruiz-Boix[1], Antonio Lozano[1], Leonardo Ariel Cano[2], Sofía Isabella Cabrera Febres[1], Lucía Navarro-González[1], Aleksandr Kovalev[1], Leili Soo[1], Ángela Bernabeu-Sanz[1], Cristina Soto-Sánchez[1] and Eduardo Fernández[1,3]

[1]Biomedical Neuroengineering Group (nBio), Instituto de Bioingeniería (IB), Universidad Miguel Hernández (UMH), 03202, Elche, Spain

[2] Neuroscience and Applied Technologies Laboratory (LINTEC), Instituto Superior de Investigaciones Biológicas (INSIBIO), Bioengineering Department, Faculty of Exact Sciences and Technology (FACET), National Scientific and Technical Research Council (CONICET), National University of Tucuman (UNT), 4000, San Miguel de Tucumán, Argentina

[3]Research Networking Center in Bioengineering, Biomaterials and Nanomedicine (CIBER-BBN), 28029, Madrid, Spain.

* These authors contributed equally (maria.mgilabert@umh.es and o.hernandez@umh.es)

Introduction: Visual deprivation can alter sensory processing beyond the visual system. Blindness may lead to cross-modal reorganization and enhanced tactile abilities. Somatosensory evoked potentials objectively measure early cortical touch responses. The N20 component (~20 ms post-median-nerve stimulation) reflects the earliest cortical somatosensory processing. We used high-density EEG to characterize N20 amplitude, topography, and source estimates, alongside resting-state alpha activity, in three participants with visual impairment. We also evaluated N20 longitudinal persistence in a blind participant with a cortical neuroprosthesis.

Methods: Two blind participants (C1, C2) and one with low vision (B1) were compared with eight controls. B1 had low vision for 5 years, C1 was blind for 3 years, and C2 had a 60-year history of blindness with a Utah array implanted in V1 for five months. Median-nerve stimulation was set to minimum intensity producing thumb movement. N20 parameters, normalized topography, sources, posterior alpha, and IRASA spectral components were analyzed. C2 recordings included preoperative/postoperative sessions and paired measurements before/after cortical stimulation. Comparisons used Crawford–Howell tests with Holm correction.

Results: Across the cohort, N20 was identified at 17–20 ms. C2 showed a baseline right-hand peak of -2.69 µV vs. -1.13 ± 0.58 µV in controls ($p = 0.028$) with 20–200 Hz filtering, whereas B1 and C1 remained within control limits. Topographic analysis using Global Field Power (GFP) revealed high similarity between normalized N20 scalp maps across participants ($r \geq 0.81$) and reproducible topography in C2 ($r = 0.94$). Over five months, C2's right-hand N20 persisted (-1.6 to -2.6 µV) across measurements. Source analysis provided no evidence of additional occipital recruitment. Visually impaired participants showed lower alpha reactivity (adjusted $p = 0.014$), and C2 exhibited lower rhythmic alpha activity (adjusted $p = 0.001$), although B1 retained a rhythmic alpha component.

Conclusions: High-density EEG enabled successful mapping of N20 topography and estimated sources. Visually impaired participants showed no additional occipital recruitment. C2 displayed a prominent right-hand N20 persisting throughout follow-up. Reduced alpha dynamics may reflect altered posterior EEG activity associated with visual deprivation, while C2's weak rhythmic alpha activity may be compatible with her longstanding blindness.

SECTION B / Neural mechanisms of artificial vision

P11

High-Density Recording and Microstimulation of the Macaque Lateral Geniculate Nucleus

Presenter Feng Wang

Feng Wang, Maureen van der Grinten, Emilie Revol, Chris Klink, Roxana Kooijmans, Florian Fallegger, Rick Schuurman, Patricija Burgar, Kate Langan, Lisa Kirchberger, Bert Monna, and Pieter R. Roelfsema

Electrical stimulation of the lateral geniculate nucleus (LGN) can evoke phosphenes, making it a target for a visual prosthesis. Useful artificial vision will require phosphenes at multiple locations in the visual field. We tested whether a high-density array could record visual responses from the LGN and evoke phosphenes at locations predicted by neuronal receptive fields. We implanted a multi-shank array in two adult male rhesus macaques (Macaca mulatta). Designed for chronic deep-brain implantation, the array comprises flexible polyimide shanks with 1,008 channels for recording and microstimulation. We recorded from monkey 1 under anaesthesia and from monkey 2 during six weeks of awake behaviour. Checkerboard stimuli evoked multi-unit responses on 171 recording channels in monkey 1 and 638 in the peak recording block in monkey 2, across multiple shanks and depths. We mapped receptive fields using dense noise and moving bars. In monkey 1, LGN microstimulation evoked responses in primary visual cortex that increased with stimulation current. We trained monkey 2 to report phosphene locations with saccades and to maintain fixation on catch trials without stimulation. Across three sessions, stimulation of 16 of 17 electrodes elicited localised saccade endpoints. For all 13 electrodes with a matched receptive field, saccade direction agreed with receptive-field direction, although the endpoints generally fell short of the receptive-field centre. The median detection threshold was 23 µA across 15 electrodes with successful psychometric fits. These results demonstrate visual recording and microstimulation in the LGN with a single high-density array. The saccade reports are consistent with localised phosphenes, supporting further development of LGN visual prostheses.

SECTION B / Neural mechanisms of artificial vision

P12

From Thalamic Stimulation to Perception: Cortical and Perceptual Detection Responses to Electrical Activation Of The Lgn

Presenter Puk Lavreeke Nuijten

P.L. Nuijten, P. Neering, C. Ray, P. Ruther, M. Asplund, P.R. Roelfsema

Electrical stimulation of the visual thalamus has been proposed as a potential strategy for restoring vision in cases of cortical blindness or retinal degeneration. Prior work in non-human primates has shown that lateral geniculate nucleus (LGN) microstimulation can evoke saccadic behavior consistent with an artificial visual percept, but it remains unclear how this artificial thalamic activation propagates through cortical circuits, and whether it can support learned perceptual detection in a more tractable rodent model. Here, we present preliminary findings investigating the impact of LGN stimulation on cortical activity and perceptual detection in mice.

We combined focal electrical stimulation of the LGN with widefield calcium imaging and two-photon imaging in mouse visual cortex (V1) to characterize cortical responses at population and cellular resolution. In parallel, mice were trained in a perceptual detection task to assess whether LGN stimulation is behaviourally detectable as a visual percept. Stimulation intensity was systematically varied to determine optimal stimulation parameters. The data presented here are preliminary and based on a single animal to date.

In this animal, electrical stimulation of the LGN reliably evoked activity in V1, with response amplitude scaling with stimulation intensity. Widefield imaging revealed structured cortical activation patterns consistent with feedforward thalamocortical propagation. At the cellular level, preliminary two-photon imaging showed selective recruitment of V1 neurons. Moreover, behavioural data from this animal indicate that it learned to detect LGN stimulation in a perceptual detection task, extending evidence for perceptually relevant artificial thalamic activation to a mouse model.

These preliminary, single-animal findings suggest that electrical stimulation of the LGN can drive cortical activity and support perceptual detection behaviour. Data collection in additional animals is ongoing to confirm these results. If replicated, these findings would support the feasibility of the visual thalamus as a target for vision restoration approaches and provide insight into thalamocortical processing mechanisms.

SECTION B / Neural mechanisms of artificial vision

P13

Visual Coding and Artificial Activation in the LGN–V1 Pathway

Presenter Rim Sadry

The lateral geniculate nucleus (LGN) is a thalamic relay that conveys retinal input to the primary visual cortex (V1) and shapes early visual processing (Sherman & Guillery, 2002; Briggs & Usrey, 2007). Although direct stimulation of the LGN can generate visual percepts (Pezaris & Reid, 2007), the relationship between LGN activity and its cortical representation remains poorly understood. This question is critical for developing thalamic visual prostheses, where artificial stimulation must reliably engage cortical circuits.

We therefore investigate the LGN from two complementary perspectives: its response to natural visual input and the cortical consequences of its artificial activation. Using two-photon calcium imaging, we first characterize LGN population responses to visual stimulation, establishing how visual information is represented within the thalamic relay. We then optogenetically activate LGN relay neurons while recording neuronal responses in V1, providing a direct measure of how artificial thalamic activity is transmitted to the cortex. By linking the functional representation of visual stimuli in the LGN to the cortical responses evoked by direct LGN activation, our approach aims to identify how thalamic activity is transformed across the LGN–V1 pathway. These results provide a framework for understanding the cortical impact of artificial LGN stimulation and for designing more targeted strategies for thalamic visual restoration.

SECTION B / Neural mechanisms of artificial vision

P14

Optogenetic Stimulation in the Macaque Lateral Geniculate Nucleus: Acute Electrophysiological Validation

Presenter Prithu Purkait

Prithu Purkait, Florian Fallegger, F. Arcizet, C. Klink, E. Zin, M. Anquetil, R. Sadry, R. Arab, V. Fradot, C. Bradic, G. Labernede, A. Fayard, S. Lecourtois, J. Flament, R. Aron-Badin, D. Dalkara, Serge Picaud, Pieter Roelfsema

Visual prostheses based on electrical stimulation are limited by spatial resolution and lack of cell-type specificity. The lateral geniculate nucleus (LGN) is a compact, retinotopically organized relay between the eye and V1, that offers a promising target for optogenetic stimulation. This project tests whether optogenetic LGN stimulation can drive controlled neural activity, working towards spatially precise artificial percepts. Two macaques received intra-LGN AAV injections expressing CoChR and ChrimsonR (expression confirmed histologically, reported separately). In two terminal experiments, a 32-channel linear probe was advanced through multiple grid locations/depths (19-25.8 mm from dura) spanning the LGN. Multiunit (MUA) and single-unit activity were recorded during visual flicker and optogenetic stimulation (470/575 nm LEDs; ramped power, pulse width, frequency). Visual flicker evoked multi-unit activity consistent with probe placement in LGN. Optogenetic stimulation evoked short-latency MUA and single-unit responses time-locked to individual pulses (Fig. 1), with amplitude increasing with optical power, consistent with opsin-driven activation. These acute recordings show optogenetic stimulation can drive LGN activity in a power-dependent manner. We are now developing a chronic implant system combining a microLED probe along with a flexible electrode, for simultaneous stimulation and recording in awake, behaving animals, to quantify LGN-evoked artificial percepts with behavioural output.

SECTION C / Prosthetic vision perception and rehabilitation

P15

PhosLab: A Computational Platform for Phosphene Mapping in Cortical Visual Implants Using Anatomical Models and AI

Presenter Lillian Isabel Ocampo Fernández

Lillian Isabel Ocampo Fernández[1], José Manuel Ferrández Vicente[1], Eduardo Fernández Jover[2], Antonio Manuel Lozano Ortega[2]
[1] Universidad Politécnica de Cartagena (UPCT), ETSII, Cartagena, Spain
[2] Instituto de Bioingeniería, Universidad Miguel Hernández (UMH), Elche, Spain

Cortical visual prostheses aim to restore rudimentary vision in blind individuals, yet phosphene position, size and persistence vary considerably across users. Implant design, percept simulation, psychophysical mapping and map optimization are still handled in separate, manual workflows, which limits the personalization of retinotopic maps.

Here we present PhosLab, a computational platform that integrates this workflow in a single graphical interface. Its Implant Explorer module, built on vimplant2 and the Benson retinotopic atlas, allows for the placement of Utah-, Comb- and Thread-type arrays and exports receptive-field coordinates. The Percept Mapper module renders phosphenes with a biologically plausible model derived from Dynaphos and records participant reports through a graphics tablet or eye tracking, using randomized, practice and catch trials. Bayesian and neural (MLP) modules correct the resulting maps.

As an internal technical validation, five experiments were conducted with three volunteers from the development team, evaluating localization error as a function of eccentricity, input device, implant geometry and mapping method, as well as recovery of a known injected bias. Simulator noise was disabled except in Exp. 5, so errors mainly reflect participant response precision. We measured localization error versus eccentricity (median 0.255°, 199 valid trials; $r = 0.254$, $p < 0.001$), compared the graphics tablet with eye trackers (Pupil Core, 0.828°; Pupil Neon, 2.065°; $p < 0.0001$), and quantified visual field coverage by implant geometry, with arrays placed on the platform in layouts used in practice (Thread-1024, 68.36 deg²; Comb, 3.63 deg²; Utah, 1.20 deg²). Mapping methods were compared (absolute, 0.255°; relative, 0.525°; forced adjustment, 1.247°; $p < 0.0001$). Error reduction by the Bayesian and neural correctors was assessed against a synthetic linear bias of 2.236° (89.2% and 91.3%, respectively).

PhosLab offers a reproducible, open-source and experimentally validated framework that reduces the fragmentation between anatomical prediction, phosphene simulation and map optimization. Next steps include validation with real intracortical stimulation data, more participants, and closing the learning loop across sessions.

SECTION C / Prosthetic vision perception and rehabilitation

P16

Security-Aware Scenario-Based Operational Vocabulary

Presenter Estela Díaz-López

David Bernal-Casas [0000−0002−4623−5935], Mariano Rincón [0000−0002−0138−4662], Estela Díaz-López [0000−0001−6448−7741] and Margarita Bachiller [0000−0001−9122−0858]
Department of Artificial Intelligence, Universidad Nacional de Educación a Distancia (UNED), Madrid, Spain
{ dbernal, mrincon , ediazlopez,marga}@dia.uned.es

Background: Visual neuroprostheses can evoke phosphenes through controlled stimulation, but current optimisation strategies primarily focus on identifying effective stimulation patterns rather than converting induced percepts into reliable units of information. Subjective responses may differ in valence, intensity, clarity, temporal stability and spatial configuration. We propose a security-aware framework for constructing an individualised operational vocabulary from reproducible phosphene experiences while explicitly accounting for perceptual uncertainty and potentially unpleasant stimulation. Methods: Trial-level stimulation parameters will be integrated with affective ratings, verbal descriptions and available annotations concerning percept intensity, clarity and spatiotemporal stability. The proposed protocol comprises four stages. First, supervised models will examine the association between stimulation parameters and perceptual valence to identify configurations associated with pleasant, neutral or unpleasant responses. Second, semantic representations and unsupervised clustering will be used to detect recurrent perceptual classes, such as almond-shaped, rice-grain-shaped, linear, arc-like, star-like or diffuse percepts. Third, percepts satisfying predefined criteria for comfort, reproducibility and discriminability will be assigned unique operational codes. Fourth, the resulting subject-specific vocabulary will be evaluated in scenario-based tasks in which sequences of stimulation codes convey elementary information through previously learned percepts. Safety constraints will exclude aversive or unstable patterns from the operational vocabulary. Results: The framework defines a reproducible pathway from heterogeneous subjective reports to a structured and safety-filtered perceptual lexicon. Its evaluation will quantify class stability, between-trial reproducibility, perceptual separability, decoding accuracy and the frequency of ambiguous or adverse responses. Validation in a new participant will determine whether stimulation-to-percept associations can support reliable recognition of coded sequences under controlled experimental conditions. Conclusions: A security-aware operational vocabulary could extend visual stimulation research beyond stimulus optimisation towards the controlled encoding of information through reproducible artificial percepts. If experimentally validated, this approach may provide a foundation for personalised phosphene-based communication, perceptual training and future visual brain-computer interfaces.

SECTION C / Prosthetic vision perception and rehabilitation

P17

An Augmented Reality Platform for Comparing Simulated and Actual Prosthetic Vision

Presenter Maureen van der Grinten

Restoring functional vision means restoring the ability to interact with the world in real time, recognising people and objects, and navigating independently. Simulated prosthetic vision has yielded valuable insights into which image-processing approaches, electrode layouts and stimulation strategies produce interpretable and functionally useful percepts. However, by design it is tested only in sighted humans, leaving the question of how well its predictions transfer to real prosthetic vision.

Here, we describe the development and initial validation of an augmented reality platform designed to bridge this gap in nonhuman primates. We redirect vision to a monitor which can display a real-time camera feed of the environment in front of the monkey with artificial elements overlaid. This includes the space where the monkey can use its hands to interact with the physical world. We use an integrated MATLAB experimental control package and Unity-based rendering pipeline to control the visual scene in this AR environment. We trained one monkey (rhesus macaque) to perform an object identification and grasping task. A custom, motorised turntable was used to position objects at different locations. The monkey then performed visual search to identify and interact with the physical 3D object. Initial testing shows that the mirror-based AR system allows for a wide field of view and accurate eye-tracking, minimizing distortion of the visual field. The full image processing and rendering pipeline is closed loop with minimal latencies (<60ms) and at high frame rates (60Hz). The turntable allows for millisecond precision of hand logging. These macaques are implanted with high-density electrode arrays, allowing for hybrid phosphene-physical interactions. This setup allows for one-to-one comparison of simulated to actual prosthetic vision.

SECTION C / Prosthetic vision perception and rehabilitation

P18

Neurovision: A wireless Virtual Reality Platform for Mobility-Oriented Prosthetic Vision Simulation

Presenter María del Mar Ayuso Arroyave

Maria del Mar Ayuso Arroyave, Antonio Lozano, Roberto Morollón Ruiz, Aimee Solzbacher, Cristina Soto-Sánchez, Leili Soo, and Eduardo Fernández

Visual neuroprostheses require realistic simulation tools to evaluate stimulation strategies before clinical translation. However, current prosthetic vision simulators are often limited to desktop environments, single implant models, or static experimental conditions. We present NEUROVISION, a modular wireless virtual reality platform for real-time simulation of low vision and visual neuroprostheses during active exploration. The system integrates a PICO 4 Enterprise headset with a Python-based server through a Unity/C# client-server architecture, enabling gaze-contingent processing of live passthrough video.

NEUROVISION supports cortical and retinal prosthesis models, visual pathology simulation, configurable image preprocessing, eye tracking, object detection, obstacle segmentation, doorway detection, and mobility-oriented phosphene patterns. Recent developments also include optimized threaded communication, asynchronous detection modules, headset-motion logging, and per-eye gaze-pose recording. Preliminary validation demonstrated stable operation across most simulation modes, calibrated eye-tracking accuracy of approximately 0.48°, and quantitative mobility analysis from four walking recordings comprising 1,789 samples, 212.4 s of movement, and 118.1 m of accumulated trajectory. The main performance bottlenecks were complex retinal simulation and semantic detection modules.

These results support NEUROVISION as a flexible experimental platform for studying prosthetic vision, low-vision assistance, and navigation-oriented visual restoration strategies in immersive and mobile VR conditions.

SECTION C / Prosthetic vision perception and rehabilitation

P19

Point-SPV: end-to-end Enhancement of Object Recognition in Simulated Prosthetic Vision Using Synthetic Viewing Points

Presenter Ashkan Rahmani Nejad

Prosthetic vision systems aim to restore functional sight for visually impaired individuals by replicating visual perception by inducing phosphenes through electrical stimulation in the visual cortex, yet there remain challenges in visual representation strategies such as including gaze information and task-dependent optimization. In this project, we introduce Point-SPV, an end-to-end deep learning model designed to enhance object recognition in simulated prosthetic vision. Point-SPV takes an initial step toward gaze-based optimization by simulating viewing points, representing potential gaze locations, and training the model on patches surrounding these points. Our approach prioritizes task-oriented representation, aligning visual outputs with object recognition needs. A behavioral gaze-contingent object discrimination experiment demonstrated that Point-SPV outperformed a conventional edge detection method, by facilitating observers to gain a higher recognition accuracy, faster reaction times, and a more efficient visual exploration. Our work highlights how task-specific optimization may enhance representations in prosthetic vision, offering a foundation for future exploration and application.

SECTION C / Prosthetic vision perception and rehabilitation

P20

The Impact of a Linear Ground Texture on Distance Estimation in Simulated Phosphene Vision

Presenter Eleftherios Papadopoulos

Eleftherios Papadopoulos, Julia Verhij, Rob van Lier, Arno Koning, Yagmur Güçlütürk

Visual prosthetic devices can offer a novel perceptual tool to blind individuals by electrically stimulating the visual system to produce perceptions of spots of light known as phosphenes. These phosphenes can be patterned strategically through scene processing algorithms to represent visual information. However, current devices produce limited, low-resolution percepts that are insufficient for many everyday tasks, including depth perception and navigation. The present study evaluated a ground theory-inspired scene processing strategy that overlays the ground plane with depth-conforming longitudinal lines, represented as rows of phosphenes that increase in density and decrease in size with distance. This texture was designed to provide depth cues analogous to those identified in J.J. Gibson's ground theory of space perception. Using a biologically plausible cortical implant simulation, 29 sighted participants completed a depth interval bisection task in a simulated three-dimensional virtual reality environment, in which they adjusted the position of a middle block to the perceived midpoint between a near and far reference block. Three scene processing modes were compared: the proposed Depth-Lines condition, a Canny edge detection control (Edges-Only), and a fixed vertical line control (Fixed-Lines). A Bayesian mixed effects model revealed that the Depth-Lines condition produced significantly lower errors than both control conditions across several distance and object width configurations, with the greatest advantage observed when objects were closer to the viewer, when greater intermediate ground space was visible, when size constancy cues were unavailable, and when the distance between objects exceeded the high-resolution foveal region, requiring reliance on the low-resolution peripheral phosphene field. These findings provide evidence that a ground texture conforming to depth can partially counteract the intrinsic bias toward distance underestimation present in phosphene vision.

SECTION C / Prosthetic vision perception and rehabilitation

P21

Blind People Guidance Using Area Center Algorithm

Presenter Félix de la Paz López

José Manuel Cuadra Troncoso Francisco Antonio Marín García Félix de la Paz López José Ramón Álvarez-Sánchez
Artificial Intelligence Dept. UNED (Spain)

We seek inspiration in the way humans solve the problem of finding the right path while avoiding obstacles. For example, when we hurry across a busy street. At each stage of the journey, we reactively scan our surroundings and follow the center of the open space around us. Crowded areas cause us to look down and, consequently, slow down; conversely, open areas allow us to look up and thus increase our speed. These ideas led to the area center algorithm and have been applied to reactive navigation for autonomous robots in previous work, in which distances to surrounding obstacles were measured using lidar or depth cameras. When the center of the zone is near an obstacle or within it, the algorithm divides the detected zone into two parts and uses one of the two area centers for guidance. Our algorithm also enables robots to reach targets reactively by using other sensors to detect them. In this study, we propose using the area center method to help blind people walk safely and reach their destinations using information extracted from the algorithm, see figure 1. We have enhanced the algorithm for detecting steps, stairs leading down and cliffs to warn the users so they can avoid them or help them get down. Outdoors, information about destinations can be obtained via GPS, and indoors, via low energy Bluetooth beacons (BLE). If maps of the surrounding area are also available, improved versions of the algorithm will allow users to follow complex paths to reach their destination. The users will wear AI-powered glasses, a device equipped with depth cameras. The position of the area center and other information will be indicated via implants in the visual cortex, binaural sounds, etc.

SECTION C / Prosthetic vision perception and rehabilitation

P22

Oculomotor Stability Predicts Phosphene Perception in a Blind Participant with Cortical Visual Neuroprosthesis

Presenter María del Mar Ayuso Arroyave

Maria Del Mar Ayuso Arroyave, Leili Soo, Odelaysis Hernández, Avi Caspi and Eduardo Fernández

Cortical visual prostheses can evoke phosphenes through intracortical electrical stimulation, but their functional use may depend on the interaction between perception, spatial localization, and oculomotor instability. We analyzed eye-tracking and behavioral data from a blind participant with bilateral cosmetic ocular prostheses, nystagmus, and an implanted cortical visual prosthesis. Eye movements were recorded with Pupil Core during cue-following, phosphene localization, vestibulo-ocular reflex testing, and two phosphene psychophysics sessions.
Video-based pupil re-detection was used to improve signal quality over the raw Pupil Capture output. The participant showed intermittent jerk-like nystagmus, marked asymmetry between eyes, and a hypoactive but compensatory vestibulo-ocular reflex. Across experimental sessions, the participant consistently localized perceived phosphenes to the left side of space using a manual ball-positioning task (88/95 responses, 92.6%). However, gaze direction was not reliably aligned with either the cued side or the reported phosphene location.

In the psychophysics sessions, phosphene reports occurred mainly with ambient light on, whereas light-off sessions nearly abolished phosphene perception. Pre-stimulus ocular stability predicted perception: in the right eye, greater nystagmus velocity during the 1-s pre-stimulus window reduced the odds of reporting a phosphene (OR = 0.65, 95% CI 0.49-0.86, p = 0.003), controlling for stimulation amplitude. By contrast, stimulation did not produce a robust immediate modulation of nystagmus.

These findings suggest that, in this participant, oculomotor instability may represent an additional constraint on reliable phosphene perception. These findings motivate testing gaze-stability–contingent stimulation as a strategy for improving perceptual reliability in cortical visual neuroprostheses.

SECTION C / Prosthetic vision perception and rehabilitation

P23

Crowding at an Eccentric Locus: Location-Specific Perceptual Learning And Its Implications for Visual Rehabilitation After Implantation

Presenter Elena von Perponcher

Elena von Perponcher, Mark W. Greenlee, Herbert Jägle, Tina Plank

Background. Peripheral vision is limited by crowding: an object identifiable in isolation becomes hard to identify when similar objects fall within a critical spacing. Individuals with central vision loss (CVL), a candidate population for visual prostheses, rely on peripheral vision for everyday tasks such as reading. Many develop a preferred retinal locus (PRL) in the intact peripheral retina. We asked whether crowding can be reduced by perceptual learning, whether learning depends on the trained locus, and whether it transfers to everyday tasks.

Methods. Fifteen CVL patients and 15 age-matched controls trained 8 days on a Landolt C gap-orientation task with two radial or two tangential flankers; the outcome was critical target-flanker spacing. Patients trained at the PRL and at an equally eccentric, unused control retinal locus (CRL) in intact retina; controls at matched coordinates under central fixation. Acuity, Vernier hyperacuity, contrast sensitivity, word recognition and reading speed were measured before and after training. As PRL eccentricity varied, critical spacings were expressed as Bouma factors (b) and converted to V1 distance (Horton & Hoyt, 1991).

Results. Both groups improved significantly at both locations. Before training, patients showed more crowding at the CRL than at the PRL (b = 0.72 vs. 0.50), whereas controls did not differ between matched locations (0.33 vs. 0.33). Training reduced the cortical critical distance at the PRL from 6.9 to 4.8 mm (-30%), and at the CRL from 9.0 to 7.5 mm (-17%). Radial-tangential anisotropy was found in controls but not in patients. Transfer to word recognition was significant in patients only at their PRL, and reading speed improved in patients. Acuity, hyperacuity and contrast sensitivity were unchanged after training.

Conclusions. Performance on crowding tasks in CVL is trainable, but learning and transfer are strongest at the established PRL, suggesting that plasticity is preferentially allocated to the locus already in use. A previously unused locus of equal eccentricity (CRL) improved less and did not close the gap to the PRL within 8 days. For prosthetic vision, competition with an established PRL may need to be addressed in post-implantation rehabilitation.

SECTION D / Neural interfaces stimulation technology and biocompatibility

P24

Towards A Flexible, Deep, High-Channel-Count Electrode Array for Cortical Visual Prosthetics

Presenter Emilie Revol

Emilie Revol, Feng Wang, Antonio Lozano, Carter Kelly, Pavlo Zolotavin, Yuhang Ma, Chris Klink, Chong Xie, Pieter Roelfsema

Blindness affects approximately 40 million people worldwide and profoundly limits independence and quality of life. Retinal prostheses can restore limited vision but are ineffective when the eye-to-brain pathway is damaged or degenerated. Direct electrical microstimulation of visual cortex is a promising alternative, evoking phosphenes that may be combined to generate meaningful visual patterns. However, clinical translation is constrained by two challenges: rigid silicon/metal electrodes induce gliosis and encapsulation, degrading the electrode-tissue interface and long-term performance; and sufficient visual-field coverage is difficult since large regions of human primary visual cortex are buried within sulci, inaccessible to existing implants. To address these limitations, this work focuses on the development of a highly flexible, high-channel-count cortical implant, with implantation strategies enabling deep and distributed placement along sulci. We are developing a 1024-channel implant, comprising 16 probes of 7 long, highly flexible polyimide shanks each (14 mm; 112 shanks total). The long shanks are designed to reach neurons along the lunate sulcus in monkeys (as a proxy for the calcarine sulcus in a human surgical approach to reach V1), and target multiple visual areas (V1, V2, V3 and V4). A custom insertion system was engineered, incorporating tungsten shuttles for temporary mechanical stiffness and a motorized insertion driver offering precise control of trajectory, depth, and velocity. Validation experiments confirmed that the custom insertion system enabled reliable, precise placement of the flexible shanks. Micro-CT imaging of monkey cadaveric brain tissue confirmed appropriate insertion and retention of the shanks in the tissue following shuttle retraction and demonstrated the feasibility of implanting 16 probes in close proximity. These findings were further supported by the ability to record visually evoked neural responses following implantation of such probes in an anesthetized monkey. Collectively, these results support the feasibility of the proposed implant architecture and implantation strategy for cortical visual prostheses targeting neurons along sulci and allowing multi-area stimulation and recording in monkeys.

SECTION D / Neural interfaces stimulation technology and biocompatibility

P25

Inter-Shank Spacing as a Key Factor in the Spatial Organization of Cortical Tissue Responses to Flexible Intracortical Electrodes

Presenter Lucía Navarro-González

Lucía Navarro-González, Adrián Villamarin-Ortiz, Cristina Soto-Sánchez, Patrick Ruther, and Eduardo Fernández.

Background and objective: Flexible intracortical electrodes offer opportunities to improve neural interface integration, but tissue responses also depend on device geometry. In multishank arrays, reduced inter-shank spacing may promote interactions between responses surrounding neighboring shanks. We compared 400 and 200 µm spacings to assess the magnitude and spatial organization of astroglial, microglial and neuronal labeling.

Methods: Flexible four-shank arrays with 400 µm (n = 3 animals) or 200 µm (n = 2 animals) spacing were implanted unilaterally in adult Wistar rat visual cortex. Tissue was collected 3 weeks after implantation, with the contralateral hemisphere serving as an internal control. GFAP, Iba1 and NeuN immunofluorescence quantified marker-positive area across cortical depth. Additional analyses assessed distances from shank edges to peak labeling across individual shanks and cortical layers, and normalized signal distributions within corridors between adjacent shanks.

Results: Both configurations showed increased GFAP and Iba1 labeling compared with contralateral controls. The 200 µm configuration showed greater depth-integrated GFAP-positive area than the 400 µm configuration. No significant differences between spacings were detected in depth-integrated Iba1 or NeuN measures. Within the analyzed profiles, all three markers showed peak labeling closer to shank edges at 200 µm, with variations across shanks and cortical layers. Corridor maps showed more continuous normalized GFAP and Iba1 distributions at 200 µm, consistent with greater spatial overlap of glial labeling. The 400 µm configuration showed more spatially segregated patterns. NeuN labeling showed spatial differences without establishing spacing-dependent neuronal loss.

Conclusions: This proof-of-concept study suggests that inter-shank spacing is associated with the magnitude and spatial organization of cortical tissue responses to flexible intracortical electrodes. At 200 µm, greater depth-integrated astroglial labeling accompanied closer peaks within the analyzed profiles and more continuous normalized glial labeling between shanks. Future studies will expand animal cohorts to assess reproducibility and depth dependence, and combine histological analyses with electrical stimulation to investigate how spacing and stimulation jointly influence tissue responses and functional outcomes.

SECTION D / Neural interfaces stimulation technology and biocompatibility

P26

Changes in Myelin Morphology Following Penetrating Electrode Array Implantation in Peripheral Nerves.

Presenter Gloria Ruiz-Boix

Gloria Ruiz-Boix[1]*, Gema Martínez-Navarrete[1], Sonia Andreu-Vera[1], Andrea Rodríguez-Despaigne[1], David Warren[2] and Eduardo Fernández[1]
[1]Biomedical Neuroengineering Group, Institute of Bioengineering, Miguel Hernández University, Elche, Spain
[2]Department of Biomedical Engineering, University of Utah, Salt Lake City, Utah, USA
*gloria.ruiz@goumh.umh.es

Background: Implantation of penetrating neural interfaces can produce heterogeneous changes in myelin morphology that may not be fully captured by conventional fiber classifications. We characterized peripheral nerve tissue remodeling and fiber morphology following Utah Slanted Electrode Array (USEA) implantation at 7 and 28 days post-implantation, focusing on non-degenerated fibers with intermediate myelin morphology.

Methods: Histological, morphometric, and ultrastructural analyses were performed on 15 sciatic nerve samples from adult Sprague-Dawley rats, including non-implanted controls and nerves collected 7 or 28 days after pneumatic or manual USEA implantation. Conventional classification included mature myelinated, hypomyelinated, and degenerated fibers. Profiles with intermediate myelin morphology were analyzed either within the hypomyelinated category, following the conventional approach, or as a separate descriptive category. The g-ratio (axon diameter/total fiber diameter) and ultrastructural myelin lamellar organization were assessed.

Results: Intermediate profiles were scarce at 7 days but more abundant at 28 days in both implantation groups. At 28 days, their g-ratio values distinguished them from mature myelinated and hypomyelinated fibers. Field-emission scanning electron microscopy (FESEM) of 28-day post-implantation samples showed an intermediate degree of myelin organization, with an average of 17.949 ± 0.364 myelin lamellae, intermediate between mature myelinated and hypomyelinated fibers. To assess the analytical value of retaining intermediate profiles separately, the two classification approaches were compared at 28 days. Under the conventional classification, no differences between implantation methods were detected among non-degenerated fibers. However, when the intermediate profiles were retained separately, their density was higher in the pneumatic than in the manual group (18,775.5 vs. 8,163.3 fibers/mm^2; $p = 0.0005$).

Conclusions: These findings indicate that penetrating electrode array implantation is associated with heterogeneous changes in peripheral nerve myelin morphology and suggest that retaining intermediate profiles as a separate descriptive category may provide complementary analytical resolution for characterizing this response.

CONCLUSIONS: These findings indicate that penetrating electrode array implantation is associated with heterogeneous changes in peripheral nerve myelin morphology and suggest that retaining intermediate profiles as a separate descriptive category may provide complementary analytical resolution for characterizing this response.

SECTION D / Neural interfaces stimulation technology and biocompatibility

P27

Hybrid Electrical and Optical Visual Cortical Prosthesis

Presenter Peimin Yuan

Visual prostheses aim to restore vision by modulating neural activity in the visual pathway and generating phosphenes that can be assembled into biomimetic visual perception. Electrical cortical stimulation provides fast response and low power consumption, but its selectivity is limited by current spread and lack of cell-type specificity. Optogenetic stimulation offers cellular specificity and spatial control, but is constrained by light scattering, slower response and high optical energy demand. To address these limitations, we propose a hybrid electronic and optogenetic visual cortical prosthesis combining subthreshold electrical and optical stimulation. The central concept is a three-dimensional stimulation structure in which neural activation occurs only at the intersection of the electrical and optical fields, improving spatial selectivity while reducing optical energy. In this work, we present modelling, hardware implementation and preliminary in vivo validation of the proposed system. Biophysical neuron simulations evaluated the feasibility of dual-mode stimulation. The model showed that neither subthreshold optical nor electrical stimulation alone evoked an action potential, whereas their combination successfully activated the target neuron. Under the tested condition, hybrid stimulation reduced activation energy by approximately 29.3% compared with optical-only stimulation. To support experiments, we developed a prototype platform integrating a multi-channel current driver, LED driver, recording amplifier and filter, power management and user-interface-based parameter control. Preliminary animal experiments used cortical stimulation and eye-tracking-based behavioural readout. Electrical stimulation of the visual cortex elicited observable behavioural responses, demonstrating that the hardware can deliver stimulation and support behavioural assessment. Although the dataset remains limited, these results confirm system functionality and feasibility, providing a foundation for future studies with larger sample sizes and more rigorous evaluation of hybrid optogenetic–electrical stimulation strategies.

SECTION D / Neural interfaces stimulation technology and biocompatibility

P28

Closed-Loop Neural Stimulation for Visual Prosthetics

Presenter Xiyuan He

Xiyuan He, Tibor Rózsa, Ján Antolík, Jichun Li, Patrick Degenaar

Visual prostheses provide a potential neuroengineering approach for restoring limited visual perception by bypassing damaged visual pathways and stimulating the visual cortex. However, conventional open-loop stimulation cannot monitor the actual neural response, making it difficult to compensate for variability, noise and response delay. This project develops a closed-loop neural stimulation framework for visual brain prostheses, using an AdExp spiking neural network model of the primary visual cortex to simulate cortical responses to stimulation. The system continuously measures neural activity and adjusts stimulation based on the error between the target and measured response. Results show that closed-loop control improves target-response tracking, reduces response delay and lowers stimulation energy compared with open-loop stimulation. These findings suggest that closed-loop stimulation can provide more accurate, faster and more efficient neural coding, supporting more stable visual feature representation in future visual prosthetic systems.

SECTION D / Neural interfaces stimulation technology and biocompatibility

P29

A Hardware-Enforced Safety Envelope for Ml-Driven Intracortical Stimulation

Presenter Marta Gea Ponce

Alicia Aniorte, Marta Gea, Javier Garrigós, José M. Ferrández

BACKGROUND. Closed-loop cortical visual prostheses increasingly rely on encoders that set per-electrode stimulation in real time. These encoders are opaque and retrained as they evolve, so their behaviour cannot be exhaustively verified, yet their output could reach tissue with no clinician in the loop: automated stress testing of published encoders reports out-of-limit stimulation under perturbed inputs. In practice this risk is contained either by restricting the encoder to a small set of pre-validated configurations, as in early intracortical trials, or by firmware and hardware safeguards that clip or drop out-of-range parameters. Both act per command and per parameter: neither bounds a quantity that only exists over a pulse train or across channels, such as accumulated charge per electrode or neighbourhood co-activation. METHODS. We propose a safety envelope in programmable logic, interposed between controller and output stage with no bypass path, enforcing pre-validated clinical limits whatever the controller commands. Verification is split across three domains of the refinement chain, each with an independent monitor and disjoint fault coverage: T1 checks the commanded parameters, T2 the generated waveform and T3 the delivered stimulation. T1 and T2 are dissimilar by abstraction, not technology: one predicts injected charge from the command, the other counts cycles on the waveform, and both must agree exactly.

Fig. 1. Placement of the T1, T2 and T3 verification points along the closed-loop stimulation pipeline. RESULTS. T1 has been implemented in synthesisable C++ (Vitis HLS) as an AXI peripheral for a Zynq-7020. Constraints are organised along two independent axes, scope (single electrode vs. neighbourhood) and time (single pulse vs. full sequence), yielding four constraints. T1 returns a per-electrode execution mask and applies to any stimulator, including closed commercial chips; T2 additionally requires an observable generator and is the next implementation phase, together with the T3 audit of delivered charge. CONCLUSIONS. Enforcement placed downstream of the controller and locked independently of it bounds any encoder version without re-establishing the safety argument after each retraining. T1 provides an immediate command-level baseline while T2 and T3 close the remaining gaps between commanded, generated and delivered stimulation.

SECTION D / Neural interfaces stimulation technology and biocompatibility

P30

HEMI-FLASH-RED: a Red-LED Flash VEP Stimulator With Hemifield Stimulation and EEG Synchronisation

Presenter Julia Paredes de Isla

Flash visual evoked potentials (VEPs) allow the visual pathway to be assessed in patients who cannot cooperate, as well as during surgery that puts it at risk, such as procedures involving the sellar region or the optic chiasm. However, conventional flash stimulators illuminate the entire visual field, which limits lesion localisation, and their synchronisation with the recording system is often poorly controlled.

To address these limitations, HEMI-FLASH-RED is presented, a system that combines stimulation goggles with their control unit, an EEG amplifier, protocol management software and visualisation software that tracks VEP amplitude and latency against a baseline. Each eyepiece holds 48 red 635 nm LEDs that stimulate through the closed eyelid, split into two 24-LED hemifields so that the nasal and temporal retina can be stimulated independently. Flashes are timed on board, and a hardware TTL pulse marks every flash in the EEG, making timing independent of the wireless link.

This hemifield design is the main innovation. Since nasal fibres cross at the chiasm while temporal fibres do not, comparing both responses may help distinguish prechiasmal, chiasmal and retrochiasmal lesions. In addition, a wireless, battery-powered version integrated into the frame is intended for use in the operating room, enabling real-time monitoring of the visual pathway during surgery.

The electronic design, firmware and protocol software have been completed. Next steps include photometric and timing characterisation of the stimulus, validation in healthy volunteers and evaluation in intraoperative monitoring, addressing response stability under anaesthesia as well as battery and radio safety under the EU Medical Device Regulation 2017/745.

SECTION E / Neural decoding brain machine interfaces and research tools

P31

Beyond Simple Movements: Premotor Cortex Enables Adaptive BMI Control

Presenter Alessia Sepe

Alessia Sepe[1], Sofie De Schrijver[1], Irene Caprara[1] ,Ophelie Saussus[1], Renaud Detry[2,3], Pinhao Song[2], Thomas Decramer[4], Peter AJ Janssen[1]
[1]Laboratory for Neuro- and Psychophysiology, Department of Neurosciences, KU Leuven, Leuven, Belgium
[2]Research unit Robotics, Automation and Mechatronics, Department of Mechanical Engineering, KU Leuven, Leuven, Belgium
[3]Research unit Processing Speech and Images, Department of Electrical Engineering, KU Leuven, Leuven, Belgium
[4]Research Group Experimental Neurosurgery and Neuroanatomy, KU Leuven, Leuven, Belgium

Intracortical brain-machine interfaces (BMIs) are typically evaluated in simple, predictable environments. Yet real-world applications require flexible control under changing environmental demands. Which cortical populations support this adaptability remains unclear.

We simultaneously recorded neural activity from primary motor cortex (M1), ventral premotor cortex (PMv), and dorsal premotor cortex (PMd) using three 96-channel Utah arrays in macaques controlling an avatar through an online BMI. Animals navigated immersive 3D virtual environments of increasing complexity, from unobstructed target-directed movements to navigation with obstacles, viewpoint changes, and cluttered scenes. The decoder was trained exclusively during passive observation of simple target-directed movements.

Despite increasing task demands, animals maintained stable BMI performance without decoder retraining. Unexpected obstacle appearance elicited robust modulation in PMv, while M1 and PMd were comparatively unaffected. Gaussian Process Factor Analysis revealed globally conserved population trajectories across tasks, accompanied by area-specific geometric changes: increasing complexity was associated with higher-dimensional dynamics in PMv and PMd, whereas M1 dynamics became lower-dimensional, with changes dominated by trajectory offsets. To assess the functional contribution of each region to BMI control, we selectively excluded its signals from decoding. M1 signals alone supported control in simple environments, whereas successful adaptation to complex environments increasingly depended on premotor signals.

Together, these findings reveal a task-dependent redistribution of cortical contributions to BMI control. They suggest that incorporating premotor signals may be particularly valuable for intracortical interfaces designed to operate in dynamic, unpredictable environments.

SECTION E / Neural decoding brain machine interfaces and research tools

P32

ImaDec: Visual Imagery Decoding from V1 of a Blind Participant

Presenter Lorenzo Russo

I plan to present a transformer-based architecture that predicts the color imagined by a blind participant. The model uses multi-unit activity extracted from V1 signals recorded using a Utah Array. The model outperforms baseline regression models and can be adapted to new data, including online recordings, through fine-tuning. A closed-loop protocol in which the participant is informed of the prediction improves overall performance.

SECTION E / Neural decoding brain machine interfaces and research tools

P33

Learning Continuous Representation from Raw Intracortical Recordings

Presenter Diogo Berger Monteiro

Diogo Berger Monteiro and Aleksandr Kovalev, Aitor Morales-Gregorio, Lorenzo Russo, Adrian Villamarin-Ortiz, Fabrizio Grani, Gloria Ruiz Boix, Lucia Navarro González, Rocío López-Peco, María del Mar Ayuso Arroyave, Leili Soo, Cristina Soto Sánchez, Antonio Lozano, Eduardo Fernández

Objective. Intracortical brain-computer interfaces (BCI) typically discard information about timing and waveform of spikes due to threshold-crossing rates and spike-band power binned at tens of milliseconds. Before such feature extraction, also LFP is removed and with it additional information. This work explores how far the broadband signal can be compressed in time before losing these components.

Approach. We train a causal convolutional autoencoder to compress 30kHz spontaneous-activity from the human visual cortex, recorded using a Utah array, to 125Hz. Two decoders share the compressed signal to reconstruct the LFP across frequency bands from delta to high gamma and individual spike waveforms on a silent background.

Main Results. The signal decoder reconstructs the LFP from delta to high gamma with near-perfect correlation. With a fixed threshold rule, spike detection on the spike decoder matches detection on the raw signal in participants seen during training and exceeds it in a held-out participant, whereas the reconstructed signal alone yields fewer detected spikes.

Significance. The presented architecture unifies LFP and spike waveforms representation into a single causal latent, providing a scalable, real-time front-end for closed-loop BCI decoders and downstream neural foundation models.

SECTION E / Neural decoding brain machine interfaces and research tools

P34

Embedded Deep Learning Models Towards Low-Power Neural Interfaces

Presenter Ryan Greer

Ryan Greer[1], Charly Lamothe[1], Antonin Verdier[1], Brice Bathellier[1].

[1]Université Paris Cité, Institut Pasteur, AP-HP, INSERM, CNRS, Fondation Pour l'Audition, Institut de l'Audition, Paris, France.

High channel-count neural interfaces have garnered significant attention in recent years due to their clinical implications in the treatment of neurodegenerative conditions [1]. One such application of these devices are as a cortical stimulator to restore lost sensation [2,3], but a key challenge remains in the development of encoding strategies to transmit meaningful information to the cortex [4]. As these inevitably begin to incorporate deep learning approaches [5], there is an increasing requirement for efficient electronic systems to power these models in clinical implants.

This work builds on the development of Braincodec; a biomimetic model for auditory cortical stimulation. Briefly, Braincodec is an autoencoder based on Encodec by Meta [6], but with additional biologically-inspired constraints on the latent space that are introduced during training. This allows Braincodec to not only compress sound information into a two-dimensional space, but to do so in a way that emulates the behaviour of the auditory pathway, providing a solution to sound encoding for an auditory cortical prosthesis. Here, the encoder has been optimised to run on embedded hardware with strict memory requirements, utilising pruning and quantisation-aware training (QAT). Two embedded targets have been selected for implementation of the encoder, both of which are capable of real-time neural network inference with low latency and power consumption. Preliminary results indicate that acceptable Braincodec performance can be maintained after >96% reduction in the number of model parameters. The model has been implemented on the embedded targets, verifying low power consumption (< 1 mW) permitting several days of usage on a single small battery charge (e.g. 100 mAh), and at the required latency of the system (<25 ms per inference).

P35

BigParma: An Open-Source Package for Fast and Automated Probe Planning and Implant Modeling

Presenter Paolo Papale

Department of Medicine and Surgery, Neuroscience Unit, University of Parma

Electrophysiological planning translates anatomical targets into probe trajectories and implant designs. Manual modeling can require many hours of work and substantial expertise in using 3D modeling software. BigParma is a fully open-source package integrating four Blender add-ons into a sequential workflow: Brain Modeler, Probe Modeler, Probe Planner and Implant Modeler. It combines atlas-derived anatomy, configurable probes, automated trajectory optimization and implant design to reduce manual work.

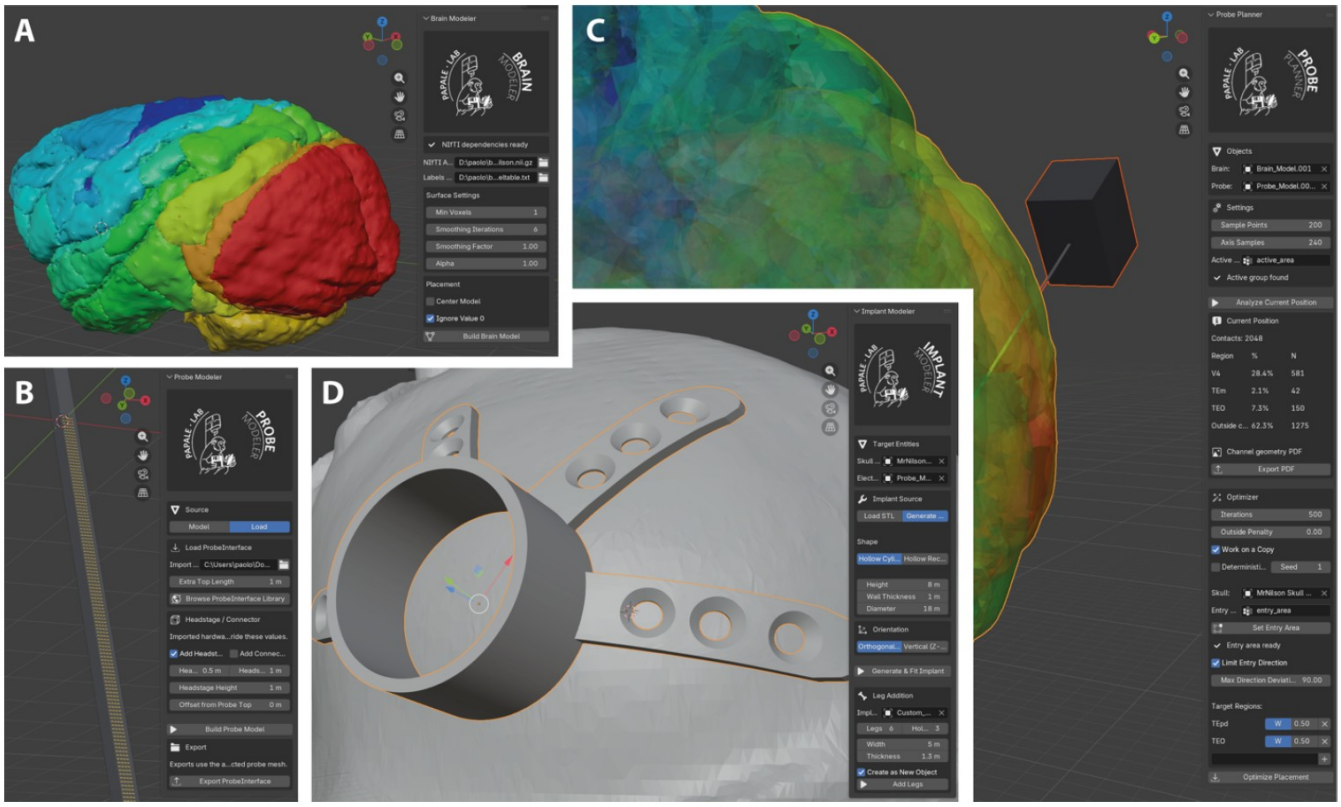
Brain Modeler converts labeled NIfTI atlases into three-dimensional brain models using TXT or CSV files that map voxel values to anatomical names (Figure 1A). Labels shared by multiple values are combined into single regions. Existing atlases thus supply the anatomical framework without requiring users to model brain structures manually.

Probe Modeler then provides the recording hardware, generating single-shank probes, multi-shank probes and two-dimensional arrays with configurable dimensions and contact layouts, plus optional headstage and connector geometry (Figure 1B). Import and export of probe descriptions support integration with existing probe libraries, reducing repetitive construction of recording-site geometry.

Probe Planner brings these anatomical and hardware models together (Figure 1C). Users select desired brain regions, assign relative priorities and define an allowed skull entry area. The optimizer automatically searches for trajectories that place recording contacts within the selected targets, refining candidate placements according to regional weights and geometric constraints. Directional limits and hardware exclusion rules constrain the search. Contact-to-region analysis and figures preserving contact geometry help users assess target coverage and compare configurations.

Implant Modeler completes the workflow by creating skull-conforming implant geometry from parametric shapes or imported STL models (Figure 1D). Mounting legs, countersunk screw holes and leg selection support adaptation to the skull and planned recording configuration.

Within one editable scene, BigParma connects anatomical atlases and probe libraries to automated trajectory planning and implant modeling. Compared with workflows requiring separate tools and extensive manual construction, this integration is designed to save hours of modeling, reduce dependence on advanced modeling skills and accelerate experimental design iteration.


A
Brain Modeler
BRAIN MODELER
Surface Settings
Placement
Build Brain Model
B
Probe Modeler
PROBE MODELER
Source
Load ProbeInterface
Build Probe Model
Export
C
Probe Planner
PROBE PLANNER
Objects
Settings
Analyze Current Position
Optimizer
Export PDF
D
Implant Modeler
IMPLANT MODELER
Target Entities
Implant Source
Shape
Orientation
Leg Addition

SECTION E / Neural decoding brain machine interfaces and research tools

P36

Generalizable Deep Learning Models for Predicting Auditory Neural Responses

Presenter Kristian Gjorgjieski

Kristian Gjorgjieski∗[1–3] , Ulysse Rancon†[2] , Marcus Jescke‡[2,4] , and Fabian Sinz§[1,2]
[1]Campus Institute Data Science, University of Göttingen, 37077 Göttingen, Germany
[2]Institute of Computer Science, University of Göttingen, 37077 Göttingen, Germany
[3]German Primate Center, 37077 Göttingen, Germany
[4]Institute for Auditory Neuroscience and InnerEarLab, University Medical Center Göttingen, 37075 Göttingen, Germany

The restoration or enhancement of sensory function with neuroprostheses requires accurate stimulation of the targeted neurons. Thus, encoding models of neuronal activity could help with the design of more principled and complex artificial stimulus patterns. The auditory system is a particularly relevant setting, as cochlear implants are among the most successful sensory neuroprostheses, and higher levels of the auditory pathway are increasingly being targeted by auditory brainstem and midbrain devices. However, quantitative models of natural-sound encoding in central auditory areas remain limited, owing to the complexity and high non-linearity of neuronal dynamics. We address this challenge with a deep-learning-based encoding model that predicts neuronal responses to natural sounds across different higher brain areas and species. While most existing machine-learning models are fitted to a single dataset, species, or recording area, our approach uses one shared architecture across different recording sites and processing stages. Specifically, we employ a three-stage design: a spectrotemporal front-end acting on the waveform, followed by a deep core module that serves as a spectrotemporal feature extractor, feeding a final readout stage trained independently for each neuron/unit to capture its individual tuning. The deep core module emphasizes a long temporal receptive field, enabling the modeling of long-timescale dynamics and post-stimulus responses, which are particularly relevant in auditory processing. We independently trained and evaluated the architecture on single-unit extracellular recordings from the marmoset medial geniculate body, ferret primary and secondary auditory cortex, and multiple zebra-finch brain areas. Our model achieved high ceiling-normalized correlations and matched or exceeded published state-of-the-art encoding models on independent benchmarks. These results suggest that a single, well-regularized architecture can provide a generalizable model of auditory neural responses across areas and species. It may therefore serve as a reusable foundation for model driven stimulus design in future central auditory prostheses, and serve as a testbed for model driven design in the visual system.

SECTION E / Neural decoding brain machine interfaces and research tools

P37

Can Shared Neural Responses Be Found Without Knowing Where to Look?

Presenter David Beinhauer

Inter-subject correlation (ISC) analysis has become a powerful tool for identifying shared neural responses to naturalistic visual and auditory stimuli [1–4]. However, most ISC studies are stimulus-informed and rely on a priori selection of time windows, electrodes, or frequency bands. It remains unclear whether shared neural responses can be recovered without such prior knowledge.

We address this question using high-density EEG from 19 participants recorded during music listening and auditory steady-state response (ASSR) stimulation, under placebo and psilocybin, with the ASSR serving as a validation condition. We search for inter-subject synchrony across full recordings without any stimulus-informed selection, applying methods of increasing complexity, from pairwise ISC and multivariate decomposition (ICA, IVA, CorrCA) to self-supervised contrastive learning.

None of the classical approaches revealed significant synchrony in either condition, including the ASSR, indicating a substantial sensitivity gap between stimulus-informed and uninformed approaches. We present a systematic comparison of the methods and preliminary results from the contrastive learning framework.

References: [1] Uri Hasson et al., Intersubject Synchronization of Cortical Activity During Natural Vision.Science303,1634-1640(2004).DOI:10.1126/science.1089506 [2] K. Lankinen, J. Saari, R. Hari, M. Koskinen, Intersubject consistency of cortical MEG signals during movie viewing, NeuroImage, Volume 92, 2014, Pages 217-224, ISSN 1053-8119, https://doi.org/10.1016/j.neuroimage.2014.02.004 . [3] Y. -P. Lin et al., "EEG-Based Emotion Recognition in Music Listening," in IEEE Transactions on Biomedical Engineering, vol. 57, no. 7, pp. 1798-1806, July 2010, doi: 10.1109/TBME.2010.2048568. [4] Daly, I. Neural decoding of music from the EEG. Sci Rep 13, 624 (2023). https://doi.org/10.1038/s41598-022-27361-x

SECTION E / Neural decoding brain machine interfaces and research tools

P38

ENGRAM: a Synchronised Platform For Neural And Media Data Visualisation

Presenter Sofía Cabrera

Objective. When stimulating and recording from a patient's brain, neurotechnology researchers are left with a huge amount of data to analyse afterwards. Every day brings several experiments, and every experiment follows its own routine. Acquiring the data is only part of the problem, because what comes after can turn into a very complicated analysis. Keeping every output organised is important, and so is having the right tools to visualise it. Approach. An engram is the trace a memory leaves in the nervous system. In the same way, Engram keeps a trace of every experiment: a synchronised platform for neural and media data visualisation where any session can be revisited and re-analysed at any time. Engram scans the data folder and organises it by patient, date, experiment and run. It also places every stream (neural signals, video, pupil, audio and trial events) on a single timeline anchored to the neural recording clock. Main results. The result is a userfriendly local platform that imports new patient recordings without ever modifying the originals, so their integrity is preserved. It scans every experiment, gives a summary of its status, flags data problems, and opens each file in the right tool for its modality. The app was tested with the complete dataset of one patient, close to a million files, to catch any inconsistency. Significance. Engram makes it possible for researchers to analyse their data in depth, more efficiently and in less time, by bringing every part of an experiment together in one place instead of scattered across folders and separate tools.

SECTION E / Neural decoding brain machine interfaces and research tools

P39

Multimodal Platform for MRI-Guided TMS Data Integration and 3D Visualization in Phosphene Research.

Presenter Geraldin Sthefany Saavedra Tafur

Geraldin Sthefany Saavedra Tafur, Leili Soo, Eduardo Fernandez Jover

MRI-guided Transcranial Magnetic Stimulation (TMS) is used to investigate visual cortex function through neuronavigation and phosphene induction. However, these experiments generate heterogeneous datasets, including neuronavigation coordinates, coil orientation, MRI scans, stimulation parameters, and subjective phosphene reports. Managing these data across multiple software environments makes integrated visualization and exploratory analysis challenging. Therefore, we developed a Python-based desktop platform that centralizes patient, session, and trial data within a unified workflow. Additionally, the application takes MRI scans in DICOM format and reconstructs them into participant-specific 3D brain models, while BrainSight-exported stimulation coordinates are projected onto the cortical surface along with coil orientation. Each trial is linked to synchronized video clips, participant drawings, and perceptual descriptors, including phosphene occurrence, brightness, and perceived size. The platform was applied to data from six participants undergoing MRI-guided visual cortex TMS experiments. Stimulation sites were visualized on participant-specific 3D brain models using a color-coded representation of phosphene-positive, phosphene-negative, and uncertain responses. In one representative session, 52 trials (17 positive, 17 negative, and 18 uncertain) were simultaneously displayed alongside stimulation coordinates and coil orientation, enabling direct spatial comparison of perceptual outcomes within a single 3D environment. This unified visualization improved experimental traceability by consolidating anatomical, spatial, and behavioral information that was previously distributed across multiple formats. Overall, this software establishes an extensible framework for exploratory analysis in phosphene research. Future work will incorporate functional Near-Infrared Spectroscopy (fNIRS) data into the same analytical framework, enabling simultaneous exploration of stimulation location, phosphene perception, and cortical hemodynamic responses. This integration is intended to support concurrent TMS-fNIRS investigations and experimental paradigms relevant to visual neuroprosthetic research.

P40

The Problem of Responsibility Gap in AI-Based Assistive Technology

Presenter Marcin Furtak

Marcin Furtak[1], Peter König[1,2]
[1]Institute of Cognitive Science, University of Osnabrück, 49069 Osnabrück, Germany
[2]Department of Neurophysiology, University Medical Centre Hamburg-Eppendorf, 20251 Hamburg, Germany

The rapid advancements in the field of artificial intelligence (AI) have led to its increased integration into domains involving physical agency. In traditional applications utilizing AI, it is possible to draw a clear division of responsibility when analyzing the decision-action loop (Figure 1). For example, a medical doctor can analyze the results of a brain scan with a machine learning model trained to search for atypical patterns; however, the final decision about how to proceed with treatment is fully on a doctor. On the contrary, when using autonomous cars, passengers can provide information about the intended destination, but the loop of subsequent decisions and preceeding actions required to reach the goal are within the scope of the car.

In the context of modern assistive technology, the division of responsibility can be unclear. For example, when analyzing HANS, the assistive system for visually impaired that helps in grasping, we notice a split of a decision-action loop across the human-AI dyadic system boundary. In this case, the user performs hand movements based on decisions made by AI-based system that processes high-dimensional signals from the environment and transforms them into navigational cues. This enables users to achieve goals unreachable without the system's assistance (i.e., grasping a desired target object). However, as a result, the boundaries of responsibility become blurred, creating a gap that makes it difficult to define a singular deciding agent, generating a critical problem for ethics of assistive technology.

The problem of the responsibility gap is likely to grow with the ongoing developments in the field of AI-based assistive devices. While the issue is important for any such technology, it is crucial in the context of invasive solutions where even physical boundaries between elements of the dyad would be blurred. Thus, we postulate the development of a new ethical framework that would take into account the shared agency of the user and AI-based system and enable assessment of responsibility within such dyadic setups. This step is essential for the assessment of accountability when developing and using novel AI-based assistive technology.

SECTION F / Neuroethics neurorights and legal responsibility

P41

PROTECTING NEURODATA: Neurorights Liability Under Article 82 of the GDPR and Other Instruments

Presenter María Remedios Guilabert Vidal

INTRODUCTION: Recent developments in science—particularly in medicine, materials science, and computing—have fostered extraordinary progress in neurotechnologies. First, this paper addresses the current state of the field, highlighting both the remarkable advances it offers for medicine and other disciplines and the serious ethical and legal challenges it presents. Undeniable progress has been made in the diagnosis and treatment of—and the improvement of quality of life for—individuals suffering from severe disorders of the nervous and musculoskeletal systems, such as blindness, Parkinson's disease, Alzheimer's disease, tetraplegia, severe depression, and ALS. It is also worth noting the wide range of neurotechnologies currently available that interact with the human nervous system, including electroencephalography (EEG), functional magnetic resonance imaging (fMRI), neurostimulators, and brain-computer interfaces (BCIs). This research focuses specifically on brain-computer interfaces and the risks they pose regarding the protection of "neuro-data"—a category of particularly sensitive information. To better understand the issues at hand, we will briefly outline the concept, types, and functioning of brain-computer interfaces. These devices connect biological reality—the brain—with a computer or even a mobile phone to record and/or modulate brain activity; consequently, the term "brain-machine interfaces" is arguably more accurate. Fundamentally, a distinction is drawn between invasive and non-invasive interfaces—depending on whether or not they require implantation in the user's body—and between those that record and/or modulate brain activity. Regarding functionality, devices that record brain activity can even decode brain patterns with the aid of artificial intelligence, making them particularly controversial. Brain-computer interfaces, for their part, may be either invasive or non-invasive. Also noteworthy is the existence of devices intended for healthcare purposes alongside those designed for wellness or entertainment, with the latter being freely available to consumers. These latter neurotechnologies raise issues of particular concern, given that some of them alter brain activity without medical supervision, in addition to the questions they pose regarding the protection of consumer neurodata—especially concerning vulnerable population groups.

SECTION F / Neuroethics neurorights and legal responsibility

P42

De las Señales Neuronales a la Prueba Jurídica: Neuroderechos y Garantías Procesales ante las Interfaces Cerebro-Computador Intracorticales

Presenter María Concepción Rayón Ballesteros

Introducción: Las interfaces cerebro-computador intracorticales están evolucionando desde sistemas experimentales hacia aplicaciones clínicas capaces de registrar, decodificar y estimular la actividad neuronal. Aunque se desarrollan para restaurar funciones perdidas, sus resultados también podrían fundamentar inferencias sobre la percepción, la intención, el reconocimiento o la memoria. Las propuestas sobre neuroderechos identifican la privacidad mental, la libertad cognitiva, la identidad y la integridad mental, pero todavía no ofrecen reglas suficientemente operativas para la utilización probatoria de los datos neuronales.

Método: La investigación combina el análisis funcional de las interfaces intracorticales con los estándares europeos sobre derechos fundamentales, protección de datos y proceso justo. Los resultados neuronales se clasifican atendiendo a su origen —espontáneo o provocado—, nivel de procesamiento —dato bruto, derivado o inferido algorítmicamente—, finalidad, voluntariedad y distancia inferencial respecto del hecho que se pretende probar.

Resultados: La capacidad técnica de acceder o decodificar una señal neuronal no determina la legitimidad de utilizarla como prueba. Se propone un marco integrado por cuatro exigencias: validez científica y cuantificación del error; consentimiento específico, informado y revocable; trazabilidad, integridad y auditoría independiente de la obtención y procesamiento; y contradicción efectiva, igualdad de armas y protección frente a la autoincriminación. Los resultados terapéuticos o asistenciales deben distinguirse de las inferencias sobre veracidad, memoria, conocimiento o culpabilidad, respecto de las cuales las tecnologías actuales no pueden proporcionar una prueba autónoma.

Conclusiones: Los neuroderechos no deben operar únicamente como un catálogo abstracto, sino como límites aplicables al diseño y utilización de las tecnologías durante todo el ciclo de vida de los datos neuronales. La integración de la privacidad y la integridad mental con las garantías procesales permite preservar la innovación clínica y evitar que las interfaces neuronales se conviertan en instrumentos no controlables de vigilancia cognitiva o de obtención coactiva de pruebas.